Dalton Transactions

ROYAL SOCIETY OF CHEMISTRY

PAPER

View Article Online
View Journal | View Issue

Check for updates

Cite this: *Dalton Trans.*, 2024, **53**, 1469

Synergy of redox-activity and hemilability in thioamidato cobalt(III) complexes for the chemoselective reduction of nitroarenes to anilines: catalytic and mechanistic investigation†

Dimitra K. Gioftsidou,[a] Michael G. Kallitsakis,[b] Konstantina Kavaratzi,[a] Antonios G. Hatzidimitriou,[a] Michael A. Terzidis,[c] Ioannis N. Lykakis *[b] and Panagiotis A. Angaridis *[a]

Reduction of nitro-compounds to amines is one of the most often employed and challenging catalytic processes in the fine and bulk chemical industry. Herein, we present two series of mononuclear homoleptic and heteroleptic Co(III) complexes, *i.e.*, $[Co(L^NS)_3]$ and $[Co(L^NS)_2L^1L^2]^{x+}$, respectively (x = 0 or 1, L^NS = pyrimidine- or pyridine-thioamidato, L^1/L^2 = thioamidato, phosphine or pyridine), which successfully catalyze the transformation of nitroarenes to anilines by methylhydrazine. The catalytic reaction can be accomplished for a range of electronically and sterically diverse nitroarenes, using mild experimental conditions and low catalyst loadings, resulting in the corresponding anilines in high yields, with high chemoselectivity, and no side-products. Electronic and steric properties of the ligands play pivotal role in the catalytic efficacy of the respective complexes. In particular, complexes bearing ligands of high hemilability/lability and being capable of stabilizing lower metal oxidation-states exhibit the highest catalytic activity. Mechanistic investigations suggest the participation of the Co(III) complexes in two parallel reaction pathways: (a) coordination-induced activation of methylhydrazine and (b) reduction of nitroarenes to anilines by methylhydrazine, through the formation of Co(I) and Co-hydride intermediates.

Received 7th September 2023,
Accepted 12th December 2023

DOI: 10.1039/d3dt02923a

rsc.li/dalton

Open Access Article. Published on 21 2023. Downloaded on 2026/4/8 04:51:27.
This article is licensed under a Creative Commons Attribution-NonCommercial 3.0 Unported Licence.

Introduction

Reduction of nitro-compounds to amines is one of the most often employed, and usually challenging, catalytic processes in fine chemical synthesis and production of important industrial precursors.[1] A number of heterogeneous catalytic systems has been developed and successfully utilized for this transformation, which, however, suffer from significant limitations.[2,3] These are mainly related to the scarcity and high cost of the employed noble-metal catalysts as well as their toxicity (due to the additives often used).[4–8] Moreover, poor selectivity in the case of functionalized nitro-compounds is frequently a major issue.[9]

For the above reasons, the quest for novel homogeneous catalytic systems which rely on the low-cost and low-environmental impact, earth-abundant 3d-metals that can mediate the reduction of nitro-compounds to amines selectively and under mild conditions is gaining growing interest.[10] In this context, a method successfully and widely used for this transformation is Béchamp's reduction, which involves the use of Fe powder in concentrated HCl(aq). However, the utilization of harsh reaction conditions and the generation of toxic waste, in combination with the lack of functional group selectivity, suggests the imperative need for more economical and efficient methods.

To that end, efficient molecular catalysts based on 3d-metal ions have recently been developed. In general, structures and physicochemical properties of transition metal molecular catalysts, and, therefore, their catalytic activity, can be tuned *via* selection of ligands with appropriate stereochemical and electronic properties or the metal itself,[11] so that they can catalyze efficiently a particular catalytic transformation, such as the selective reduction of nitroarenes ($ArNO_2$) to anilines ($ArNH_2$). A number of transition metal complexes that catalyze this transformation *via* catalytic hydrogenation has been reported. However, they mainly rely on noble metals,[12,13] and only a few

[a]*Laboratory of Inorganic Chemistry, Department of Chemistry, Aristotle University of Thessaloniki, 54124 Thessaloniki, Greece. E-mail: panosangaridis@chem.auth.gr*
[b]*Laboratory of Organic Chemistry, Department of Chemistry, Aristotle University of Thessaloniki, 54124 Thessaloniki, Greece. E-mail: lykakis@chem.auth.gr*
[c]*Laboratory of Chemical Biology, Department of Nutritional Sciences and Dietetics, International Hellenic University, Sindos, 57400 Thessaloniki, Greece*

†Electronic supplementary information (ESI) available. CCDC 1995929 (**1**), 1995931 (**3**), 1995932 (**4**), 1995933 (**5**), 1995934 (**7**) and 1995935 (**8**). For ESI and crystallographic data in CIF or other electronic format see DOI: **https://doi.org/10.1039/d3dt02923a**

Open Access Article. Published on 21 2023. Downloaded on 2026/4/8 04:51:27.
This article is licensed under a Creative Commons Attribution-NonCommercial 3.0 Unported Licence.

examples of 3d-metal molecular catalysts, such as Fe,[14–16] Mn,[17] and Co[18] complexes, have been reported. Catalytic transfer hydrogenation reactions, utilizing hydrazine derivatives, acids, or solvents as hydrogen donor molecules,[19,20] in combination with Fe,[21–23] Mn,[24] and Co[25] molecular catalysts have also been developed. In addition, $NaBH_4$ has also been used for the reduction of nitro-compounds in the presence of Fe-based catalysts.[26,27] Finally, another method that is also attracting increasing attention is catalytic hydrosilylation, due to the mild reaction conditions employed and the selectivity exhibited occasionally towards other functional groups. The most commonly used 3d-metal molecular catalysts in these reactions involve Fe,[28–32] Co,[33] Ni,[34,35] and more recently, Mn complexes.[36]

Among the least studied molecular catalysts of earth-abundant metals for the reduction of nitroarenes are those of Co. Nevertheless, owing to the ability of this metal to easily undergo three consecutive one-electron redox transformations Co(I)/Co(II)/Co(III) and to adopt both high- and low-spin electronic states, its complexes are expected to function as competent catalysts for this multi-electron redox reaction. In one of the earliest reports, Co(II) phthalocyanine (Scheme 1) was found to successfully catalyze the reduction of nitroarenes by $NH_2NH_2{\cdot}H_2O$.[37] More recently, Gupta and coworkers described the reduction of a range of different nitro-compounds by mononuclear Co(II) or Co(III) complexes bearing a tetradentate N-donor ligand, in the presence of NH_2NH_2.[38,39]

Recently, our group reported the transfer hydrogenation of nitroarenes to anilines by CH_3NHNH_2 using a tris-chelating pyrimidine-thioamidato Co(III) complex as catalyst.[40] Aiming to develop more efficient catalysts for this transformation, we extended our research endeavours in the field. In particular: (a) we synthesized new mononuclear thioamidato Co(III) complexes bearing different heteroaromatic thioamidato ligands with electron-withdrawing (EW) or electron-donating (ED) group substituents, (b) we studied the catalytic potential of these Co(III) complexes in the reduction of a range of different nitroarenes, and (c) we investigated their catalytic reaction mechanism. Generally, heteroaromatic thioamide ($L^{NH}S$) ligands offer a range of attractive features. Specifically, they have the capacity to: (a) affect the redox properties of their complexes (through their stereochemical and electronic properties), (b) exhibit hemilabile/labile coordination behaviour (acting either as terminal monodentate κS- or κN- or bidentate chelating κS,N-ligands), and (c) participate in proton transfer reactions (owing to the presence of N atoms in their heterocyclic ring that can act as protonation sites).[41–43] Therefore, the combination of these ligands with a redox-active metal center, such as Co, offer an ideal scaffold for the synthesis of robust, versatile and efficient molecular transition metal catalysts for the reduction of nitroarenes.[44,45] All complexes synthesized herein were found to be efficient catalysts for the reduction of a variety of nitroarenes to the corresponding anilines in high yields and chemoselectivity, without formation of azo and azoxy intermediates, under mild experimental conditions and low catalyst loading. Interesting structure–catalytic activity relationships were established. Finally, mechanistic investigations, using a range of different physicochemical methods, allowed us to suggest plausible reaction pathways for the catalytic transformation.

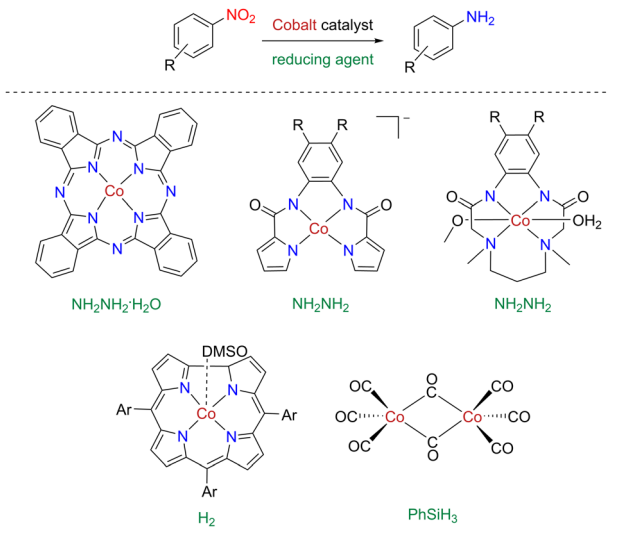

Scheme 1 Examples of molecular cobalt catalysts for the reduction of nitroarenes to anilines reported in the literature.

Results and discussion

Synthesis and characterization of thioamidato Co(III) complexes

Two series of mononuclear Co(III) complexes were synthesized: $[Co(L^NS)_3]$ and $[Co(L^NS)_2L^1L^2]^{x+}$ (x = 0 or 1), where L^NS = pyrimidine- or pyridine-thioamidato ligands bearing different EW or ED group substituents, and L^1, L^2 = phosphine, pyridine or thioamidato co-ligands (Scheme 2).

The first series of complexes comprises homoleptic tris-pyrimidine-thioamidato Co(III) complexes: [Co(pymt)$_3$] (**1**) bearing unsubstituted thioamidato ligands, [Co(tfmp2S)$_3$] (**2**) having CF_3-group substituted thioamidato ligands, and [Co(dmp2S)$_3$] (**3**) and [Co(damp2S)$_3$] (**4**) with CH_3- or NH_2-group substituted thioamidato ligands, respectively. As shown in Scheme 2, these were synthesized from reactions of $CoCl_2{\cdot}6H_2O$ with the corresponding pyrimidine–thioamide in 1 : 3 molar ratio, in the presence of $(CH_3CH_2)_2NH$, in CH_3OH, at 50–70 °C and under atmospheric conditions (Section S1.2 in the ESI†).

Views of the molecular structures of **1–4**, determined by single-crystal X-ray diffraction analysis (Table S1†), are presented in Fig. 1.[40] In all cases, an octahedrally coordinated Co(III) ion is surrounded by three chelating pyrimidine-thioamidato ligands bound through their exocyclic S and heterocyclic N donor atoms (κS,N-L^NS). Their Co–N and Co–S bond lengths fall within the ranges of 1.90–1.99 and 2.25–2.34 Å, respectively (Table S2†), indicative of low-spin, octahedrally coordinated d^6 Co(III) ions. Noticeably, **3** and **4** exhibit slightly shorter Co–S bond lengths, compared to **1**, a fact that can be attributed to

This journal is © The Royal Society of Chemistry 2024

Open Access Article. Published on 21 2023. Downloaded on 2026/4/8 04:51:27.
This article is licensed under a Creative Commons Attribution-NonCommercial 3.0 Unported Licence.

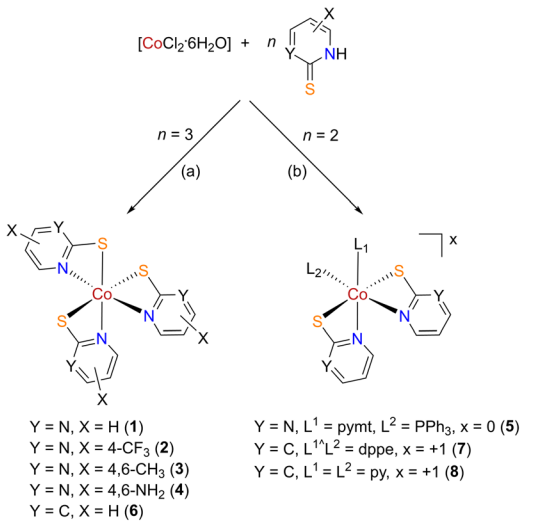

Scheme 2 Synthetic schemes and structures of complexes $[Co(L^NS)_3]$ and $[Co(L^NS)_2L^1L^2]^{x+}$ (**1–8**): (a) $(CH_3CH_2)_2NH$, 50–70 °C for 3 h under atmospheric conditions, and (b) KOH or $(CH_3CH_2)_2NH$ or CH_3ONa, 50–70 °C for 2 h under atmospheric conditions.

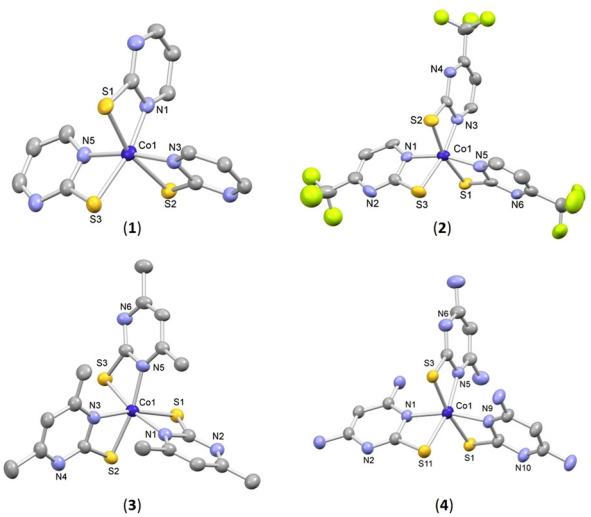

Fig. 1 Molecular structures of **1–4** as determined by single crystal X-ray diffraction. Thermal ellipsoids are drawn at the 35% probability level. All H atoms are omitted for clarity.

the ED group substituents (CH_3 and NH_2) of their ligands, which increase the basicity of their exocyclic S atom and strengthen its interaction with the metal center. In all cases, distortions from the ideal octahedral coordination geometry of the metal centers are observed (Table S2†). These are due to the small chelate ring angles of the thioamidato ligands, which result in very narrow bite angles around the metal centers. However, the sensitivity of bond angles to crystal packing forces should also not be neglected. Interestingly, the relative dispositions of the thioamidato ligands of **1**, **2** and **4** display a meridional arrangement of their respective S and N donor atoms, while in **3** a facial arrangement is observed. This variation is in accordance with examples of analogous thioamidato Co(III) complexes reported in the literature.[46–48]

FTIR spectra of **1–4** in the 4000–400 cm^{-1} region are dominated by characteristic bands of their respective thioamidato ligands. For example, **3** exhibits bands at 1580 and 1267 cm^{-1}, attributed to the C–N and the C–S bond stretch vibrations the dmp2S$^-$ ligands, respectively. ^{1}H NMR spectra of the complexes display resonances which correspond to the protons of their respective ligands (Fig. S1 and S2†). For example, **3** features one singlet for the aromatic protons of the heterocyclic rings of its dmp2S$^-$ ligands at +6.42 ppm and two singlets in the region +2.42 to +1.78 ppm attributed to the two types of CH_3-group substituents present in the complex, due to the facial arrangement of its chelating ligands. Interestingly, ^{1}H NMR spectra of all complexes remain unchanged for extended periods of time, providing an indication for their long-term stability in organic solvents.

Apart from **1–4**, heteroleptic complex $[Co(pymt)_3(PPh_3)]$ (**5**) was also synthesized (Scheme 2). This was obtained by adding to a solution of $CoCl_2{\cdot}6H_2O$ in CH_3OH a mixture of 2 equiv. pymtH and 1 equiv. PPh_3, in the presence of 2 equiv. KOH, at 50 °C and under atmospheric conditions (Section S1.2 in the ESI†). Single-crystal X-ray diffraction shows a six-coordinate Co(III) ion surrounded by two chelating κS,N-pymt, a monodentate κS-pymt, and a PPh_3 ligand (Fig. 2). The metal center exhibits distorted octahedral coordination geometry due to the steric bulk of PPh_3 ligand and the small chelate ring angles of pymt$^-$ ligands. Noticeably, Co–S bond lengths (Table S3†) are longer than those of **1–4** (average values: 2.310 *vs.* 2.280 Å, respectively). ^{1}H NMR spectrum of **5** suggests its stability in organic solvents, displaying resonances in the region +8.81 to +6.84 ppm, which correspond to the aromatic protons of thioamidato and phosphine ligands (Fig. S3†).

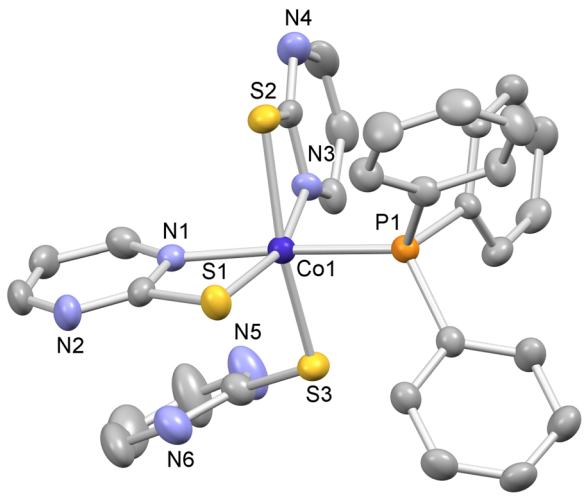

Fig. 2 Molecular structure of **5** determined by single crystal X-ray diffraction. Thermal ellipsoids are drawn at the 35% probability level. All H atoms are omitted for clarity.

Open Access Article. Published on 21 2023. Downloaded on 2026/4/8 04:51:27.
This article is licensed under a Creative Commons Attribution-NonCommercial 3.0 Unported Licence.

A series of pyridine-thioamidato Co(III) complexes **6–8** was also synthesized (Scheme 2). $[Co(2\text{-mpy})_3]$ (**6**) was obtained in a similar manner to its homologous complexes **1–4**. Its X-ray crystal structure was reported in the past and, therefore, is not discussed herein.[49–51] $[Co(2\text{-mpy})_2(dppe)]PF_6$ (**7**) was obtained from the reaction of $CoCl_2{\cdot}6H_2O$ with 2 equiv. 2-mpyH and 1 equiv. dppe in CH_3OH, in the presence of $(CH_3CH_2)_2NH$, at 60 °C and under atmospheric conditions, followed by addition of NH_4PF_6 (Section S1.2 in the ESI†). Single-crystal X-ray diffraction shows a cationic complex with its metal center chelated by two κN,S-2-mpy$^-$ and a κP,P′-dppe ligand (Fig. 3). The coordination geometry of the metal center deviates from the ideal octahedral geometry due to the combined effect of the steric bulk of dppe ligand and the small chelate ring angles of 2-mpy$^-$ ligands. Average Co–S and Co–N bond lengths are equal to 2.29 and 1.96 Å, respectively (Table S4†).[52] Finally, $[Co(2\text{-mpy})_2(py)_2]PF_6$ (**8**) was synthesized by adding to a solution of $CoCl_2{\cdot}6H_2O$ in CH_3OH 2 equiv. $Na^+(2\text{-mpy})^-$ and 1 equiv. pyridine, at room temperature and under atmospheric conditions, followed by addition of NH_4PF_6 (Section S1.2 in the ESI†). The cation of **8** consists of a Co(III) ion in a pseudo-octahedral coordination environment surrounded by two chelating κN,S-2-mpy and two py ligands at *cis* positions (Fig. 3). Average Co–S and Co–N bond lengths of thioamidato ligands are equal to 2.30 and 1.94 Å, respectively (Table S4†).

FTIR spectra of **7** and **8** confirm the presence of PF_6^- ions, as revealed by high intensity peaks at 840 cm^{-1}, which are characteristic of the ν(P–F) stretching vibrations. In the ^1H NMR spectrum of **7**, signals of the aromatic protons of the thioamidato and diphosphine ligands appear as complex multiples in the +8.39 to +6.40 ppm region, while the CH_2–CH_2 backbone of dppe appears as triplet at +1.30 ppm (Fig. S5†). For **8**, the appearance of a broad singlet resonance at +8.27 ppm is assigned to the *ortho*-protons of the pyridine ligands (Fig. S6†). Resonances of the protons of its thioamidato ligands appear in the +7.50 to +6.58 ppm range; these are shifted up-field compared to the corresponding signals of the thioamidato ligands of **7**, which bears the same thioamidato ligands and a similar structural motif.

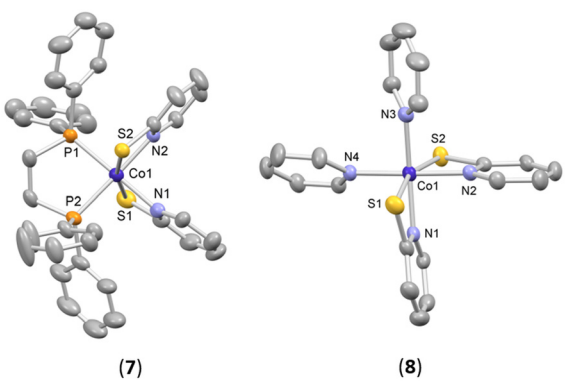

(7) (8)

Fig. 3 Molecular structures of cations of **7** and **8** as determined by single crystal X-ray diffraction. Thermal ellipsoids are drawn at the 35% probability level. Counter ions and H atoms are omitted for clarity.

Evaluation of catalytic activity

The capacity of **1–8** to catalyze the reduction of nitroarenes to anilines by CH_3NHNH_2 was studied in detail. Initial screening reactions indicated that all complexes catalyze the reaction but with different efficiencies. Optimization of the reaction conditions (solvent, temperature, time, amount of CH_3NHNH_2, and catalyst loading) was carried out using 4-nitrotoluene (**1a**) as representative nitroarene substrate and **2** as catalyst, shown to be very effective in our previous work.[40] Regarding the solvent, only polar and protic solvents were found to be suitable for the reaction, with CH_3OH promoting the total conversion of **1a** with excellent selectivity, giving *p*-toluidine (**1b**) as the only product, while CH_3CH_2OH was less effective (Table 1). Polar aprotic or non-polar solvents left **1a** completely intact. When H_2O was used, no reaction was observed, possibly due to low solubility of substrate **1a** and catalyst **2** in the particular solvent. Lowering the reaction temperature to 50 °C or shortening the reaction time to 2 h or reducing the amount of CH_3NHNH_2 to 3 equiv. resulted in lower yields of **1b**. Concerning the catalyst loading, a series of reactions were carried out using different amounts of **2**, under the same experimental conditions, and calculating the respective TONs.

Table 1 Solvent evaluation in the reduction of **1a** by CH_3NHNH_2 catalyzed by **2**

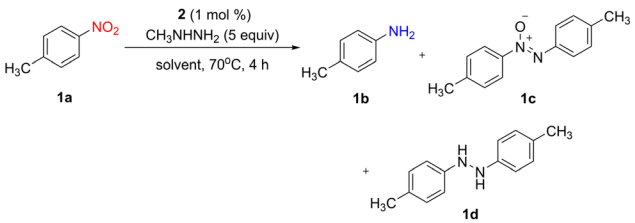

Solvent[a]	Conversion[b] (%)	1a[c] (%)	1b[c] (%)	1c[c] (%)	1d[c] (%)
CH_3OH	95	5	95	—	—
CH_3OH (2 h)	43	57	43	—	—
CH_3OH (r. t.)	—	100	—	—	—
CH_3OH (50 °C)	63	37	63	—	—
CH_3OH (3 equiv. CH_3NHNH_2)	48	52	48	—	—
CH_3CH_2OH	54	46	54	—	—
CH_3CN	<5	>95	—	—	—
$CH_3COOCH_2CH_3$	<5	>95	—	—	—
CH_2Cl_2	<5	>95	—	—	—
$OC(OCH_3)_2$	<5	>95	—	—	—
THF	<5	>95	—	—	—
Toluene	<5	>95	—	—	—
H_2O	<5	>95	—	—	—

[a] Reaction conditions: **1a** (0.2 mmol), CH_3NHNH_2 (5 equiv.), **2** (1% mol), in various solvents, at 70 °C and for 4 h in a 5 mL sealed tube. [b] Conversion percentages (%) were measured by ^1H NMR spectroscopy after addition of a specific amount of 1,3-dimethoxybenzene as internal standard. [c] Product yields were measured by ^1H NMR spectroscopy based on the integration of the appropriate proton peaks.

This journal is © The Royal Society of Chemistry 2024

Open Access Article. Published on 21 2023. Downloaded on 2026/4/8 04:51:27.
This article is licensed under a Creative Commons Attribution-NonCommercial 3.0 Unported Licence.

As shown in Table 2, the highest TON was calculated when 0.5 mol% of **2** was used. Further decrease of catalyst loading, *e.g.*, 0.2 mol%, did not lead to significant catalytic reaction, as the yield of **1b** was found to be similar to that measured for the reaction in the absence of catalyst (~10% yield). The highest TON we managed to achieve was 100, while the corresponding TOF was 25 h^{-1}.

We next compared the catalytic efficiency of **1–8** in the reduction of **1a** under the optimized reaction conditions, *i.e.*, 1 mol% catalyst, 5 equiv. CH_3NHNH_2, in CH_3OH at 70 °C and for 4 h. In all cases, *p*-toluidine (**1b**) was formed as the only product (Fig. S7–S14†). Among homoleptic pyrimidine-thioamidato Co(III) complexes **1–4**, **2** bearing EW CF_3-group substituents on its ligands was found to be the most efficient catalyst, giving almost quantitative conversion to **1b** (95% yield) (Fig. 4 and Table S5†). **1** bearing unsubstituted thioamidato ligands exhibited lower catalytic activity (65% yield), while **3** and **4**, having ligands with ED group substituents (CH_3 and NH_2, respectively), were less efficient (55% and 40% yields, respectively). These results clearly indicate the beneficial effect of EW group substituents on the thioamidato ligands in the catalytic activity of the Co(III) complexes. Interestingly, [Co(pymt)$_3$(PPh$_3$)] (**5**), bearing an additional PPh_3 ligand compared to [Co(pymt)$_3$] (**1**), displayed catalytic activity that is comparable to that of **2**, giving conversion of **1a** to **1b** in 85% yield.

Pyridine-thioamidato Co(III) complexes **6–8** were also found to be efficient catalysts, with homoleptic complex **6** exhibiting the highest catalytic activity (giving **1b** in 70% yield). Replacement of a chelating thioamidato ligand in **6** with a bulky bidentate chelating dppe ligand to give **7** resulted in significant decrease of catalytic activity (40% yield). Heteroleptic complex **8** exhibited moderate catalytic activity similar to **6** (55% yield).

It should be mentioned that under the employed reaction conditions but in the absence of any catalyst formation of **1b** was also observed, but in a negligible amount (yield < 10%, Table S5†). Also, the use of the tris-chelating Co(III) complex [Co(acac)$_3$] as catalyst also resulted in the formation of **1b** but with very low yield (Table S5†). Therefore, overall, these results clearly demonstrate the capacity of **1–8** to efficiently catalyze the reduction of **1a** by CH_3NHNH_2 giving **1b** in high yield and selectivity.

Table 2 TONs and TOFs of the reduction of **1a** to **1b** by CH_3NHNH_2 catalyzed by **2**

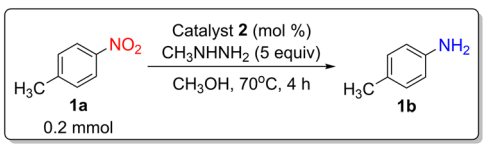

2[a] (mol%)	Conversion[b] (%)	1b[c] (%)	TON	TOF (h^{-1})
1	95	95	95	23
0.5	50	50	100	25
0.2	12	12	60	15
No catalyst	<10	<10	—	—

[a] **1a** (0.2 mmol), CH_3NHNH_2 (5 equiv.), in CH_3OH at 70 °C and for 4 h. [b] Conversion percentages (%) were measured by ^{1}H NMR spectroscopy after addition of a specific amount of 1,3-dimethoxybenzene as internal standard. [c] Product yields were measured by ^{1}H NMR spectroscopy based on the integration of the appropriate proton peaks.

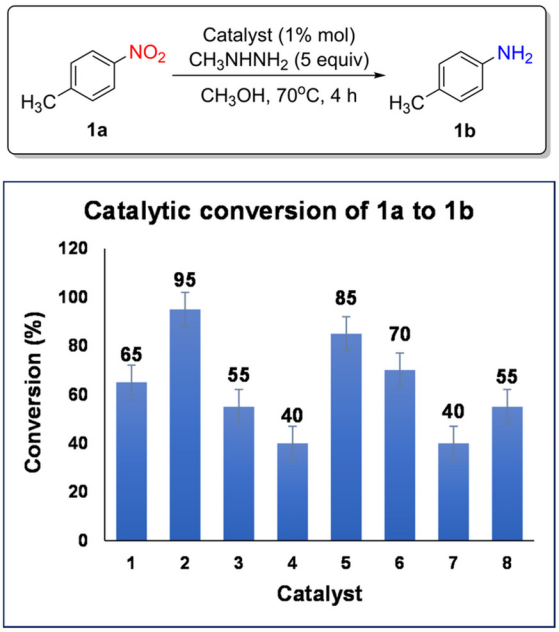

Fig. 4 Reduction of **1a** to **1b** by CH_3NHNH_2 catalyzed by **1–8** (conversion percentage are the average values of three independent experiments within 3–5% error). Conversion percentages (%) were measured by ^{1}H NMR spectroscopy after addition of a specific amount of 1,3-dimethoxybenzene as internal standard.

Synthetic application

Aiming to investigate the limits and potential of our catalytic reaction protocol, we studied the reduction of a series of variously substituted nitroarenes **1a–14a** using the best performing catalyst **2**. Our protocol was found to be successful, transforming the substrates to the corresponding amines (**1b–14b**) in moderate-to-high yields (75–86%) and with high chemoselectivity (Scheme 3). The kinetics of the reactions was found to be heavily affected by the electronic nature of their group-substituents. In particular, reduction of nitroarenes bearing ED group substituents, *i.e.*, *p*-CH_3 (**1a**) and *m*-CH_3 (**2a**), 2,3-di-CH_3 (**3a**), *p*-NH_2 (**4a**) *m*-OCH_3 (**5a**), proceeded faster and with higher product yields than those substituted with EW groups, *i.e.*, *p*-Cl (**6a**), *p*-Br (**7a**), *p*-CH_3O_2C (**8a**), *p*-$CH_3C(O)$ (**9a**), *m*-CN (**10a**) and *m*-SO_2NH_2 (**11a**). Moreover, for the latter group of substrates, prolonged reaction times (6–18 h) were required for the completion of the reaction. Importantly, the Cl- and Br-substituted nitroarenes (**6a** and **7a**) were reduced to the corresponding anilines **6b** and **7b** without undergoing reductive dehalogenation and forming the product in high yield (81%). Similarly, the CH_3O_2C, $CH_3C(O)$, CN and SO_2NH_2 functionalities in the respective nitroarenes **8a–11a** were not affected

Open Access Article. Published on 21 2023. Downloaded on 2026/4/8 04:51:27.
This article is licensed under a Creative Commons Attribution-NonCommercial 3.0 Unported Licence.

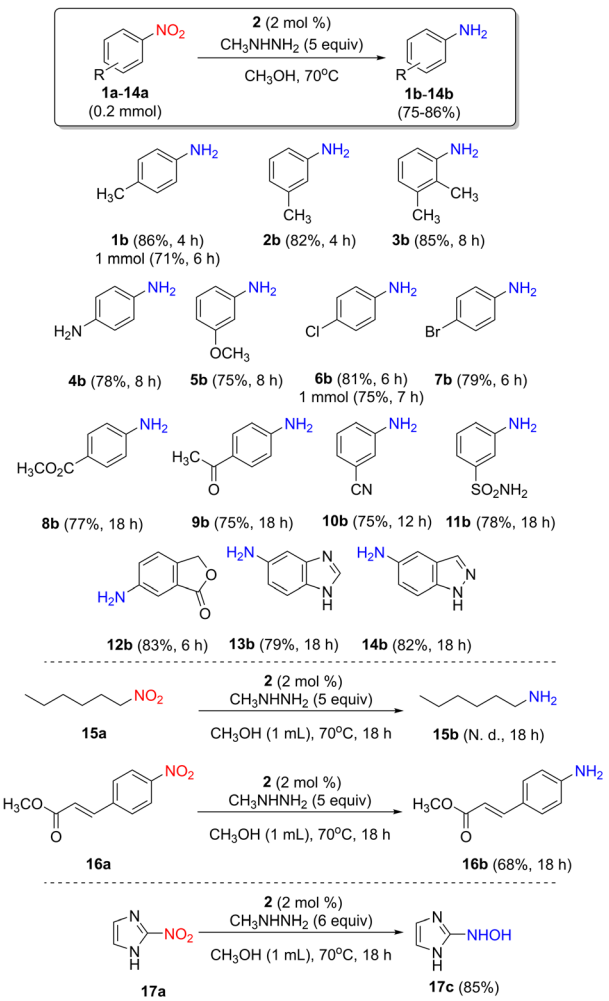

Scheme 3 Chemoselectivity of the reduction of nitro-compounds **1a–16a** by CH_3NHNH_2 to the corresponding amines **1b–14b** and **16b** as well as antibiotic **17a** to the corresponding *N*-hydroxylamine derivative **17c**, catalyzed by **2** (product isolated yield after column chromatography/appropriate time reported in parentheses). N. d. = not detected.

during the catalytic transformation, signifying highly chemoselective reactions (Fig. S15–S25†). We also examined the reduction of the heterocyclic nitroarenes 6-nitrophthalide (**12a**), 5-nitro-1*H*-benzo[*d*]imidazole (**13a**) and 5-nitro-1*H*-indazole (**14a**), resulting in the synthesis of amines **12b–14b** in high yields, 83%, 79% and 82%, respectively (Fig. S26–S28†).

In an effort to further explore the applicability of our catalytic reaction protocol, **2** was also tested in the reduction of aliphatic nitroalkane **15a** and methyl (*E*)-3-(4-nitrophenyl)acrylate **16a** (Scheme 3). Nitroalkane **15a** gave a mixture of unidentified products in *ca.* 10% conversion, in which the corresponding aliphatic amine was not observed (based on the ^{1}H NMR spectrum of the crude reaction mixture). Interestingly, **2** displayed exceptional catalytic activity towards the chemoselective nitro-group reduction of **16a**, yielding the desired amine **16b** as the major product (68% isolated yield, Fig. S29†). Remarkably, no C=C reduction was observed (based on the ^{1}H NMR spectrum of the crude reaction mixture). Therefore, these results strongly confirm the key role that **2** can play in the chemoselective synthesis of valuable amine derivatives.

Finally, we attempted the catalytic reduction of azomycin (**17a**), an antibiotic used to treat bacterial infections. Surprisingly, as revealed by ^{1}H NMR spectroscopy, the corresponding *N*-hydroxylamine derivative (**17c**) was observed as the only product (Fig. S30†). This was found to be stable under the employed reduction conditions, not getting reduced further to the desired amine even after longer reaction times. This is in agreement with our previous study on the photoreduction of nitroarenes into the corresponding *N*-hydroxylamines.[53]

Finally, to test our catalytic reaction protocol in lab-scale conditions, the reductions of **1a** and **6a** were attempted in a 1 mmol-scale, using 2 mol% **2**, in the presence of 6 equiv. CH_3NHNH_2, in 10 mL of CH_3OH at 70 °C in a sealed reaction tube. Upon completion of each reaction, the solvent was removed under reduced pressure, and, after addition of $CH_3COOCH_2CH_3$ (~15 mL), the mixture was filtered over a short silica gel pad. Following solvent evaporation, the corresponding anilines **1b** and **6b** were purified by column chromatography and isolated in yields of 71% and 75%, respectively (Scheme 3).

Mechanistic studies

The results of the catalytic activity study clearly demonstrate the high potential of heteroaromatic thioamidato Co(III) complexes **1–8** as efficient catalysts for the reduction of nitroarenes to anilines by CH_3NHNH_2, under mild reaction conditions, good product yields, high TON, and very good chemoselectivity. Ligand-effects appear to play an important role in the catalytic activity of the complexes, suggesting the existence of structure–catalytic activity relationships. Studying the correlations between the structural characteristics and physicochemical properties of the complexes with their respective catalytic activity may provide an insight into the mechanism of catalytic transformation. For this reason, a series of mechanistic investigations was conducted, using high-resolution mass spectrometry (HRMS), UV-vis absorption spectroscopy, cyclic voltammetry (CV), NMR spectroscopy and gas chromatography (GC) analysis fitted with thermal conductivity detector, as discussed below.

Structure–activity relationships. Among homoleptic pyrimidine-thioamidato Co(III) complexes **1–4**, **2** that bears ligands with EW CF_3-group substituents was found to be the most efficient catalyst, while **3** and **4** with ED CH_3- and NH_2-group substituted ligands are less active. A likely reason is the effect of the substituent groups on crucial properties of the thioamidato ligands. Generally, the small chelate angles of the bidentate thioamidato ligands lead to the formation of strained and low stability four-membered chelate rings which facilitate their hemilability or lability. Therefore, transformation of a chelating κS,N-L^{N}S ligand to a monodentate S-bound thioamidato (κS-L^{N}S) ligand might easily occur during the catalytic reaction, creating an open coordination site on the metal center for binding of CH_3NHNH_2 or the substrate.[44] This process might

This journal is © The Royal Society of Chemistry 2024

Open Access Article. Published on 21 2023. Downloaded on 2026/4/8 04:51:27.
This article is licensed under a Creative Commons Attribution-NonCommercial 3.0 Unported Licence.

be facilitated by the parallel protonation of the uncoordinated heterocyclic N atom.[44,51,54,55] The substituent groups of the thioamidato ligands may affect the ligands' hemilability and protonation affinity and, therefore, the catalytic activity of their respective complexes. For example, the CF_3-group substituents of the thioamidato ligands of **2** are expected to enhance the ligands' hemilability (due to their weak Lewis base character), rendering themselves more amenable to open a coordination site on the metal center. The electronic nature of the substituent groups of the thioamidato ligands also influences the ability of the complexes to undergo redox transformations, which are critical for the progress of the catalytic reaction, as discussed below. The fact that [Co(pymt)$_3$(PPh$_3$)] (**5**) is a better catalyst than [Co(pymt)$_3$] (**1**) can be attributed to its PPh_3 ligand. The repulsive non-bonding interactions of the phosphine's Ph groups with the three thioamidato ligands enhance the hemilability or lability of the latter and facilitate the formation of an open coordination site. Finally, the relative arrangement of the thioamidato ligands in **3** and **4** (displaying facial and meridional ligand dispositions, respectively, and both containing ED group substituents on their ligands) appears not to be a critical parameter, as the complexes display almost the same catalytic activity.

Among the pyridine-thioamidato Co(III) complexes **6–8**, the diphosphine-substituted complex **7** was found to be less efficient than **6** and **8**. At first glance, this comes in contrast to the enhancement of catalytic activity observed with the introduction a phosphine ligand in **5**. Possibly, the steric bulk of chelating dppe in **7** creates a sterically congested metal coordination environment that hinders the binding of CH_3NHNH_2 and/or the substrate. Interestingly, **8** bearing two pyridine ligands appears to exhibit similar catalytic activity to homoleptic complex **6**.

High-resolution mass spectrometry. To get an insight into the role of CH_3NHNH_2 in the catalytic reaction, its interaction with the Co(III) complexes was studied by HRMS (Fig. S32–S34†). **2** in CH_3OH gives a mass peak at *m*/*z* 634.8634, which corresponds to the molecular ion $[Co(tfmp2S)_3 + K]^+$ (Fig. S33a†). Addition of 1–2 equiv. CH_3NHNH_2 resulted in the appearance of a new mass peak at *m*/*z* 642.9634 assigned to $[Co(\kappa S,N\text{-}tfmp2S)_2(\kappa S\text{-}tfmp2SH)(CH_3NHNH_2)]^+$ (Fig. S33b†). Further addition of CH_3NHNH_2 led to the appearance of an additional mass peak at *m*/*z* 507.0031 assigned to $[Co(\kappa S,N\text{-}tfmp2S)_2(CH_2{=}NNH_2)_2]^+$ (Fig. S33c†). $CH_2{=}NNH_2$ is proposed to result from the activation of CH_3NHNH_2 upon coordination to the metal center (see below NMR spectroscopy studies).[56] Analogous results were obtained from the study of **1** and **5** (Fig. S32a–c and S34a–c†). The κS,N to κS coordination changes of a thioamidato ligand of the complexes as well as its dissociation is in accordance with its hemilabile or labile character, suggested to play crucial role in the catalytic reaction, and possibly induces a coordination activation pathway of CH_3NHNH_2 (see below in Proposed mechanism).

UV-vis absorption spectroscopy. The interaction of CH_3NHNH_2 with the Co(III) complexes was also studied by UV-vis absorption spectroscopy. UV-vis spectra of the pyrimidine-thioamidato Co(III) complexes **1–5** in CH_3OH show broad and high intensity absorptions in the high energy region with band maxima λ_{max}(abs) ~ 325 nm and $\varepsilon \sim 5000\text{–}15\,000\ M^{-1}\ cm^{-1}$, which are attributed to intraligand charge transfer (π–π*) electronic transitions (Fig. 5). Lower intensity absorptions are observed in the 400–500 nm region, which are assigned to charge transfers between the ligands to the metal center. In the 600–700 nm region all complexes display low intensity absorption bands ($\varepsilon < 300\ M^{-1}\ cm^{-1}$) attributed to d–d electronic transitions (inset in Fig. 5).[39,52,59] Among the complexes (Fig. 5 and Fig. S35†), differences in the λ_{max}(abs) of their low energy absorption bands are observed, which can be explained by differences in the Lewis base character of their respective ligands. For example, between **2** and **3**, bearing CF_3- and CH_3-group substituted ligands, respectively, the former displays a red shifted d–d absorption band, consistent with a lower ligand crystal field strength.

We followed the changes of the spectral characteristics of **2** in CH_3OH upon addition of increasing amounts of CH_3NHNH_2. Colour changes of the solution were observed (from dark brown to light brown), with concomitant changes in its d–d absorption band. Upon addition of 0.25 equiv. CH_3NHNH_2, the intensity of the d–d absorption band was reduced, while addition of 0.5 equiv. CH_3NHNH_2 resulted in its complete disappearance (Fig. 6). No further changes were observed after addition of more than 0.5 equiv. CH_3NHNH_2. Considering that 1 equiv. CH_3NHNH_2 can generate $4e^-$ and $4H^+$ before its conversion to N_2, the 1 : 0.5 stoichiometry of **2** : CH_3NHNH_2 suggests the reduction of the Co(III) complex to a lower oxidation-state Co species (possibly Co(I)). Such a species is also suggested to be formed in the catalytic reaction and participate in the reduction of the nitroarenes. An analogous spectrophotometric titration was conducted for **3**, a complex that showed lower catalytic activity. In this case, we did not discern analogous spectral changes in its d–d absorption band (Fig. S36†), a fact that might be related to the difficulty of **3** to form a reduced Co species (see below in Cyclic voltammetry).

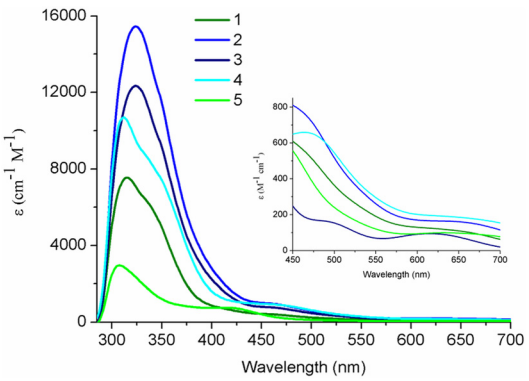

Fig. 5 UV-vis absorption spectra of **1–5** in CH_3OH (2×10^{-4} M). Spectra in the lower energy region are given in the inset.

Open Access Article. Published on 21 2023. Downloaded on 2026/4/8 04:51:27.
This article is licensed under a Creative Commons Attribution-NonCommercial 3.0 Unported Licence.

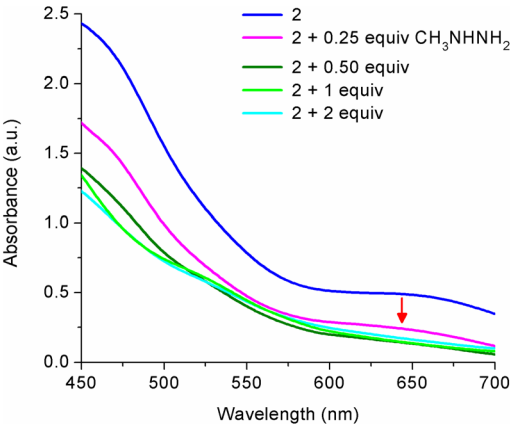

Fig. 6 Changes of the UV-vis electronic absorption spectrum of **2** in CH_3OH (3×10^{-3} M) upon progressive addition of 0.25–2 equiv. CH_3NHNH_2.

Cyclic voltammetry. To examine any correlation between the catalytic activity of **1–8** and their capability to undergo reduction to lower oxidation-state Co species, a cyclic voltammetry study was conducted. Initially, their redox behavior was examined in CH_3CN (legible data for **4** could not be obtained due to its low solubility). As shown in Fig. 7 and Table 3, all complexes undergo a reversible $1e^-$ reduction with half-wave potentials ($E_{1/2}$) in the range of −0.6 to −1.0 V, assigned to the corresponding Co(III)/Co(II) redox couples. In the −1.8 to −2.5 V range, a second quasi-reversible or irreversible reduction process is also observed which can be assigned to the corresponding Co(II)/Co(I) redox couples. The second reduction process becomes more quasi-reversible at higher scan rates (>0.1 V s^{-1}) (Fig. S39†).[44,57,58] This could be attributed to a chemical change taking place, such as change of the coordination mode of a thioamidato ligand from chelating κS,N-L^NS to monodentate κS-L^NS, which leaves an open coordination site on the reduced metal center facilitating the coordination of a Lewis base (solvent, CH_3NHNH_2 or substrate in the catalytic reaction).

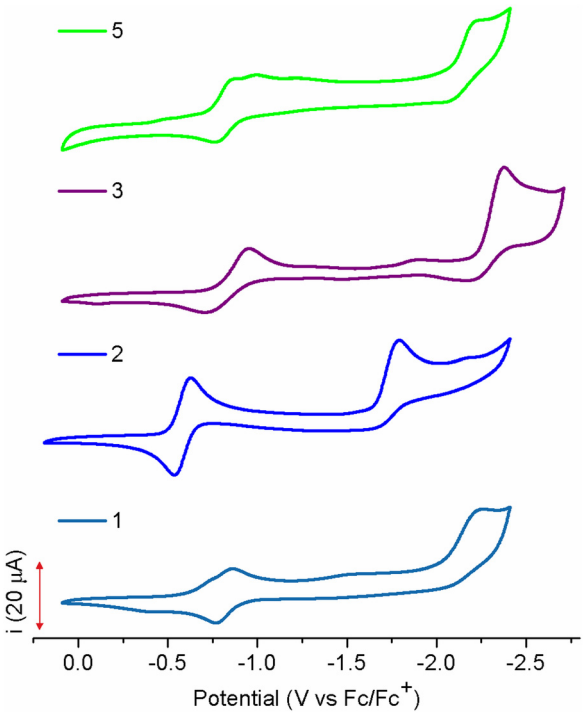

Fig. 7 Cyclic voltammograms for **1–3** and **5** in CH_3CN.

Table 3 Cyclic voltammetry data for **1–3** and **5–8** in CH_3CN

Complex	$E_{pa}^{III/II}$ [a]	$E_{pc}^{III/II}$ [b]	$E_{1/2}^{III/II}$ [c]	$\Delta E^{III/II}$	$E_{pa}^{II/I}$
1	−0.862	−0.775	−0.819	−0.087	−2.254
2	−0.629	−0.536	−0.583	−0.093	−1.790
3	−0.955	−0.717	−0.836	−0.238	−2.376
5	−0.860	−0.786	−0.823	−0.074	−2.219
6	−1.002	−0.894	−0.948	−0.108	−2.348
7	−0.971	−0.898	−0.935	−0.073	−1.778, −2.204
8	−0.998	−0.899	−0.949	−0.099	−2.451

[a] E_{pa} is anodic peak potential (V). [b] E_{pc} is cathodic peak potential (V). [c] $E_{1/2} = (E_{pa} + E_{pc})/2$. All potentials are referenced *vs.* the Fc/Fc^+ couple with $E_{1/2}(Fc/Fc^+) = 0.409$ V.

Among all complexes, **2** displays the most easily accessible Co(II)/Co(I) reduction potential (Fig. 7). This can be attributed to the EW effect of the CF_3-group substituents of its ligands, which tend to stabilize better the lower metal oxidation states.[59] Therefore, its high catalytic activity can be related to its easier access to a Co(I) species during the catalytic reaction. However, although the ease of Co(II)-to-Co(I) reduction is a factor of great importance for enhanced catalytic activity, other factors should also be favorable, such as hemilability/lability of the ligands. Indeed, **7** comes to verify this scenario (Fig. S37†): although displaying a similar redox profile with **2**, its catalytic activity is diminished.

A variable scan-rate cyclic voltammetry study was also conducted for **2** in CH_3CN (Section S2.3.3 Cyclic voltammetry†) which confirmed the homogeneous nature of the Co complexes during the redox transformations, also suggested to take place in the catalytic reduction of nitroarenes, excluding the formation of metal-based nanoparticles.

The redox behavior of **2** in CH_3CN upon addition of progressively increasing amounts of CH_3NHNH_2 was also studied. Upon addition of 1 equiv. CH_3NHNH_2, the initial redox characteristics of the complex essentially remain unaffected but two additional redox peaks also appear at −1.2 and −2.4 V (Fig. 8). The peak at −1.2 V can be attributed to the Co(III)/Co(II) redox couple of a new Co species generated from the interaction of **2** with CH_3NHNH_2 which, based on the UV-vis spectroscopy and HRMS data, possibly contains a dangling thioamidato ligand and/or a coordinated CH_3NHNH_2. The addition of more equivalents of CH_3NHNH_2 results in an increase of the height of this peak, consistent with the increase of the concentration of this new species in solution. The occurrence of the Co(III)/Co(II) reduction wave of this new species at a more negative potential than the corresponding redox wave of **2** is antici-

This journal is © The Royal Society of Chemistry 2024

Open Access Article. Published on 21 2023. Downloaded on 2026/4/8 04:51:27.
This article is licensed under a Creative Commons Attribution-NonCommercial 3.0 Unported Licence.

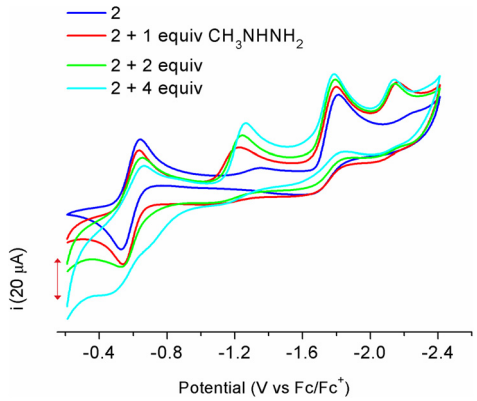

Fig. 8 Cyclic voltammograms of **2** in CH_3CN upon progressive addition of 1–4 equiv. CH_3NHNH_2.

pated, considering the strong σ-donating nature of the coordinated CH_3NHNH_2 ligands. The addition of 1 equiv. CH_3NHNH_2 also resulted in the increase of the reversibility of the Co(III)/Co(II) reduction wave of **2**, bringing the I_a/I_c ratio closer to 1 (with respect to the I_a/I_c ratio of **2** in the absence of CH_3NHNH_2). The same observation was made when the experiment was conducted in CH_3OH, the solvent of the catalytic reaction. The second new redox peak at −2.4 V appearing upon addition of CH_3NHNH_2 can be assigned to the Co(II)/Co(I) redox couple of the new species. In addition, a shift of the initial Co(II)/Co(I) reduction peak of **2** to a more accessible potential is also observed. This shift becomes greater upon increased amounts of CH_3NHNH_2 (reaching ~0.04 V at 4 equiv. CH_3NHNH_2), a result that can be attributed to the ability of CH_3NHNH_2 to provide suitable conditions in the solution (*e.g.*, solvation, polarity) to facilitate the Co(II)/Co(I) reduction.

To examine the possibility of the potential formation of a Co-hydride species and the occurrence of metal-mediated proton transfer during the catalytic reduction of nitroarenes, a CV study was conducted with **2** in CH_3CN upon addition of progressively increasing amounts of CH_3COOH as H^+ source. A new irreversible reduction wave is observed at a less negative potential than that of the original Co(II)/Co(I) redox couple (Fig. S38†).[60,61] Also, an irreversible reduction wave started growing at more negative potentials, with progressive increase of the current of the wave with increasing amounts of H^+, which is tentatively assigned to the electrocatalytically formed H_2. This behavior is typical for hydride-containing transition metal complexes that participate in proton transfer processes. Therefore, **2** in the catalytic reduction of nitroarenes to anilines has the capacity to participate in proton transfer processes (provided either by CH_3OH or CH_3NHNH_2), such as protonation of the heterocyclic N atom a thioamidato ligand or formation of a Co-hydride species, potentially key intermediates for the progress of the catalytic reaction.

NMR spectroscopy and gas chromatography studies. To probe the potential formation of a Co-hydride species during the catalytic reaction, the reduction of **1a** by **2** in the presence of CH_3NHNH_2 in CH_3OH was monitored by ^1H NMR spectroscopy. Unfortunately, we were not able to detect such species, possibly due to its low stability in the reaction medium (at least under the employed experimental conditions).[62] However, the formation of a Co-hydride intermediate is highly possible, and it has also been proposed to be formed in analogous reductive transformations by hydrazines catalyzed by transition metal complexes.[56,63]

The catalytic reduction of **1a** by **2** in the presence of CH_3NHNH_2 was also monitored by GC analysis. Analysis of the supernatant volume of gas above the reaction mixture revealed the presence of CH_4 and N_2 (Fig. S40†). The formation of these species is an immediate result of the interaction of CH_3NHNH_2 with **2**, as no evolution of gases was observed when CH_3NHNH_2 was tested under the same experimental conditions and in the absence of **2**. These results, in combination with our NMR study which showed that CH_3NHNH_2 under the same conditions is fast transformed to $CH_2{=}NNH_2$, suggest the occurrence of a CH_3NHNH_2-coordination activation pathway along with the catalytic transformation of nitroarenes (Fig. S31†). Analogous diazoalkane species were reported previously for other transition metal catalysts.[64]

Suggested reaction mechanism

Based on the results obtained from the abovementioned studies, herein we suggest a plausible reaction mechanism for the catalytic transformation of nitroarenes ($ArNO_2$) to anilines ($ArNH_2$) by **2** (the best performing catalyst) in the presence of CH_3NHNH_2. In particular, we suggest that the catalyst, apart from its participation in the reduction of nitroarenes to anilines by CH_3NHNH_2 (Scheme 5), also participates in a second reaction pathway operating in parallel, *i.e.*, coordination-induced activation of CH_3NHNH_2 (Scheme 4).

In the first step of the coordination-induced activation of CH_3NHNH_2 pathway (Scheme 4), transformation of a chelating thioamidato (κS,N-L^NS) ligand of **2** to a monodentate ligand is suggested to take place. The transformation may be assisted by the inherent hemilability of the thioamidato ligands as well as the protonation of the uncoordinated donor atom of the dangling thioamidato ligand forming a five-coordinate Co(III) intermediate ($[\mathbf{Co^{III}}]^+$). The monodentate thioamidato ligand is suggested to remain S-bound, with the most favorable protonation site being its heterocyclic N atom (κS-$L^{NH}S^+$).[51] This is in agreement with the fact that the lower oxidation-state Co species, formed in a subsequent step of the mechanism of the reduction of nitroarene by CH_3NHNH_2 (discussed below), favors the S-coordination of the ligand. Subsequently, CH_3NHNH_2 is suggested to coordinate to the $[\mathbf{Co^{III}}]^+$ intermediate ($[\mathbf{Co^{III}}$–$\mathbf{CH_3NHNH_2}]^+$). This CH_3NHNH_2-adduct can mediate the decomposition of CH_3NHNH_2 with concomitant liberation of H_2 and CH_4. Formation of H_2 might lead to a Co–($CH_3N{=}NH$) species, from which the diazene can uncoordinate restoring the $[\mathbf{Co^{III}}]^+$ intermediate. The Co–(HN=NH) species, formed upon evolution of CH_4, decomposes to N_2 resulting to a Co(III)-hydride intermediate ($[\mathbf{Co^{III}}$–$\mathbf{H}]^+$) which, upon protonation, might regenerate the $[\mathbf{Co^{III}}]^+$ intermediate. The suggestion of the coordi-

Open Access Article. Published on 21 2023. Downloaded on 2026/4/8 04:51:27.
This article is licensed under a Creative Commons Attribution-NonCommercial 3.0 Unported Licence.

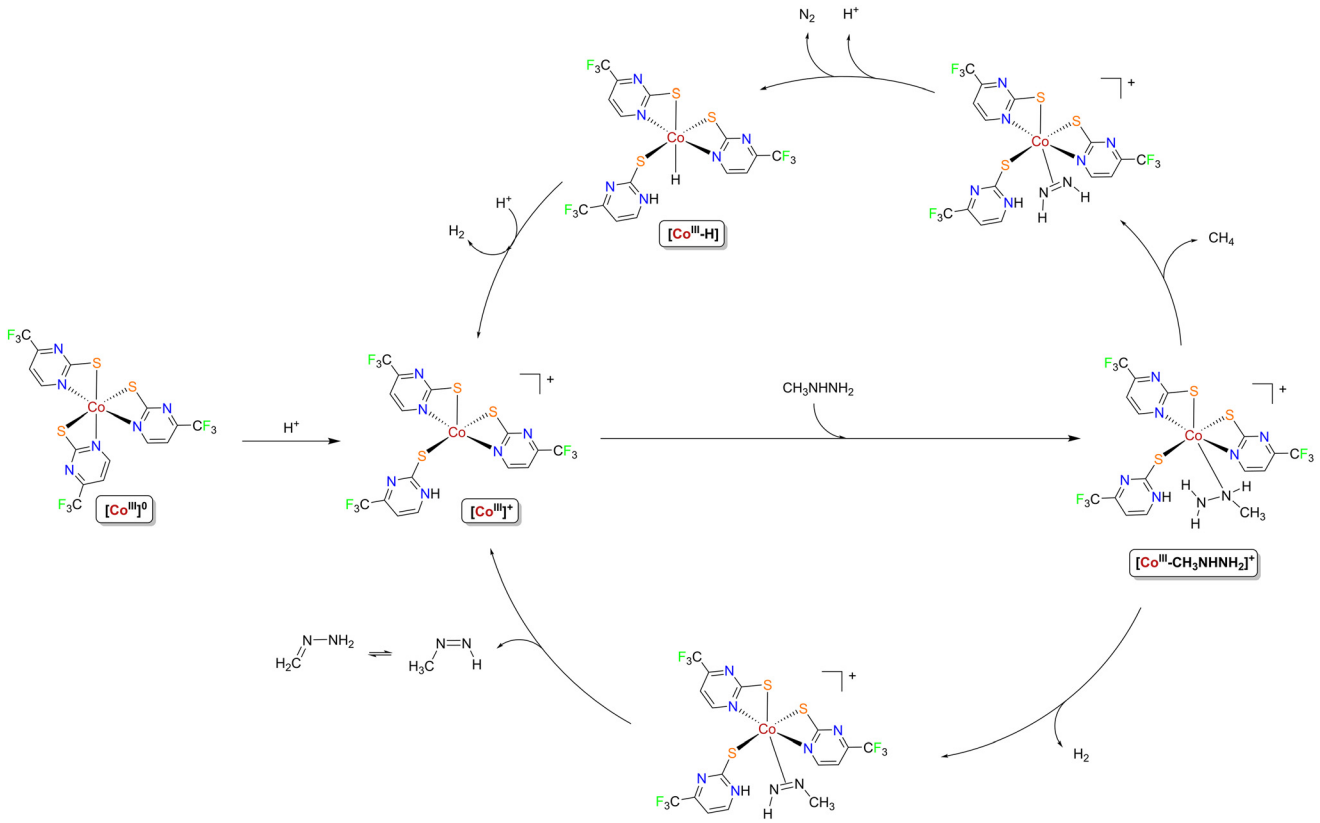

Scheme 4 Suggested mechanism of coordination-induced activation of CH_3NHNH_2 by **2**.

nation-induced activation of CH_3NHNH_2 pathway is based on the detection of the pertinent gases and the observation of $CH_2{=}NNH_2$ in the reaction mixture. Also, it agrees with recent reports on the activation of NH_2NH_2 by transition metal complexes, proposed to take place by weakening of the N–H bonds of NH_2NH_2 upon its coordination to the metal center, enabling the release of H_2 and the formation of metal-diazene and metal-hydride intermediates.[65,66]

A Co-hydride species mentioned in the abovementioned suggested pathway is suggested to be involved in the reduction of nitroarene ($ArNO_2$) to aniline ($ArNH_2$) by **2** in the presence of CH_3NHNH_2. In addition, cyclic voltammetry and catalytic activity studies suggest the importance of easy access to a Co(I)-based species for nitroarene reduction. Both species possibly play important roles in the catalytic transformation.[51,52]

Therefore, in our suggested mechanism (Scheme 5), initially, **2** ($[\mathbf{Co^{III}}]^0$) undergoes $2e^-$ reduction by CH_3NHNH_2 and protonation, leading to a five-coordinate Co(I) intermediate ($[\mathbf{Co^{I}}]^-$). This negatively charged species is expected to be stabilized by the EW CF_3-group substituted thioamidato ligands of **2**, but not by ED group substituted ligands. Considering the higher catalytic activity of **2** compared to **3** and **4** (which comprise CH_3- and NH_2-group substituents in the ligands), the particular step might have a high impact on the efficiency of the catalytic reduction. Subsequent reaction of the resulting Co(I) species with protons results in the formation of a Co(III)-hydride ($[\mathbf{Co^{III}}\text{–}\mathbf{H}]$). This intermediate is suggested to be formed *via* direct protonation of the Co(I) center and not *via* intramolecular proton transfer from the protonated thioamidato ligand to the Co center (the latter could lead to the κN,S-coordination of the thioamidato ligand which would destabilize the low oxidation state Co(I) center). Considering that hydride formation through direct protonation is expected to have high activation energy,[51] the particular step might also have an impact on the rate and efficiency of the transformation. The $[\mathbf{Co^{III}}\text{–}\mathbf{H}]$ intermediate might promote hydride transfer to the incoming substrate $ArNO_2$ (by insertion) and form a new intermediate which, upon intramolecular proton transfer from the protonated thioamidato ligand and subsequent protonation, releases H_2O. After an additional protonation, ArNHOH is released (observed experimentally as intermediate of the transformation), regenerating $[\mathbf{Co^{III}}]^0$. Intramolecular proton transfer and subsequent κN,S-coordination of the thioamidato ligand in $[\mathbf{Co^{III}}]^0$ is consistent with the stabilization of the amidato form of the ligand coordinated to a high oxidation state Co(III) center. The product of the transformation (ArNHOH) is suggested to be inserted once more in the catalytic cycle and be converted to the aniline ($ArNH_2$). It should be mentioned that the $[\mathbf{Co^{III}}\text{–}\mathbf{H}]$ intermediate, except form the abovementioned catalytic cycle, might also participate in a competitive reaction, as its direct protonation would release H_2 (Scheme 5 in the center).

This journal is © The Royal Society of Chemistry 2024

Open Access Article. Published on 21 2023. Downloaded on 2026/4/8 04:51:27.
This article is licensed under a Creative Commons Attribution-NonCommercial 3.0 Unported Licence.

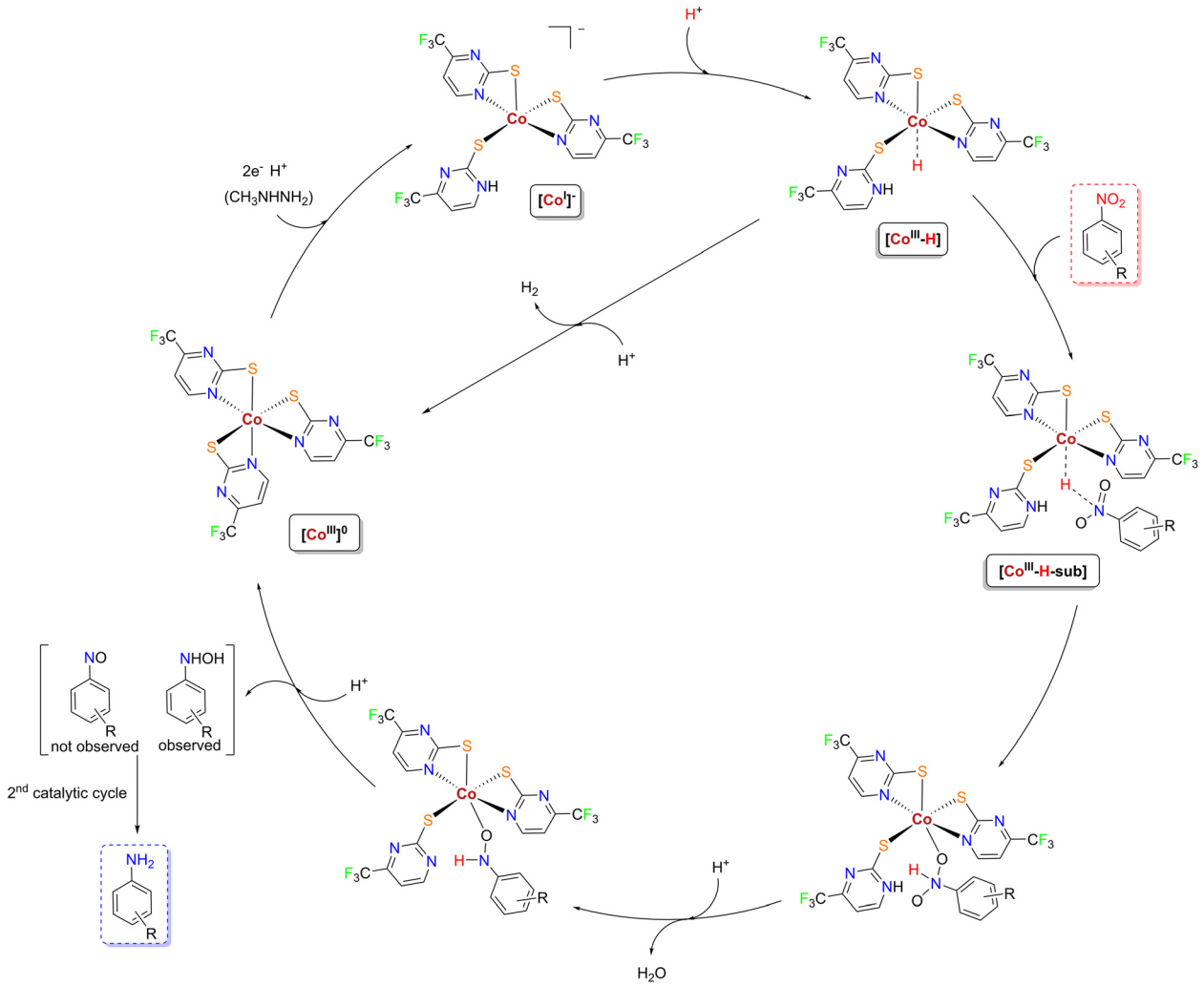

Scheme 5 Suggested mechanism of the reduction of nitroarenes to anilines by CH_3NHNH_2 catalyzed by **2**.

Generally, in the reduction of nitroarenes to anilines, the dimers azoxyarene (**1c**), and a mixture of 1,2-diphenylhydrazine (**1d**) and azobenzene may also be formed (Table 1), which are subsequently transformed to the aniline (indirect route). Although we did not detect these species in the reaction mixtures, in order to exclude their participation in the mechanism of the reaction, they were used as substrates under the employed experimental conditions. No conversion into the corresponding amines was observed, a result that supports the proposed direct route, with the reduction of nitroarenes into anilines through the corresponding observed *N*-arylhydroxylamine (ArNHOH) intermediates. Finally, nitrosoarene (ArNO) intermediates could also be formed during the catalytic reaction, which could be further reduced to the final product under either catalytic or non-catalytic conditions.[40,67] Herein, their existence was not experimentally verified; however, such reduction pathway cannot be excluded. Overall, based on the above discussion, it becomes clear that for the herein presented catalytic system of thioamidato Co(III) complexes with CH_3NHNH_2, the combination of (a) thioamidato ligands exhibiting high hemilability or lability and (b) Co(III) complexes exhibiting easily accessible Co(II)/Co(I) reduction potentials, are both essential for achieving high catalytic efficiency. These properties are more favorable in **2** (bearing EW CF_3-group substituents on its thioamidato ligands) and their synergy results in a very efficient catalyst, while in other complexes their synergy is not so efficient resulting in less effective catalysts.

Conclusions

In this work, we present two series of mononuclear Co(III) complexes bearing heteroaromatic thioamidato ligands which efficiently catalyze the reduction of nitroarenes to anilines by CH_3NHNH_2. The electronic and steric properties of the ligands of the complexes have significant impact on their catalytic activity, with complexes bearing ligands with increased hemilability/lability and/or ability to stabilize lower metal oxidation-states exhibiting higher activity. The best performing catalyst,

Open Access Article. Published on 21 2023. Downloaded on 2026/4/8 04:51:27.
This article is licensed under a Creative Commons Attribution-NonCommercial 3.0 Unported Licence.

having EW CF_3-group substituents on its thioamidato ligands, can effectively complete the transformation of a range of different nitroarenes, giving the products in high yields, high chemoselectivity and no side-products, under mild reaction conditions and using low catalyst loading. Mechanistic investigations to elucidate the role of the catalysts suggest their participation in two parallel reaction pathways: (a) coordination-induced activation of CH_3NHNH_2 and (b) reduction of nitroarenes to anilines by CH_3NHNH_2, through the formation of Co(I) and Co-hydride species.

Overall, the herein-presented results highlight the competency of the thioamidato/Co(III) scaffold in the highly efficient and chemoselective reduction of nitroarenes to anilines, and lay the grounds for its utilization in the synthesis of fine and specialty chemicals or pharmaceuticals, as well as in other multi-electron redox transformations.

Conflicts of interest

There are no conflicts to declare.

Acknowledgements

The authors kindly acknowledge financial support from the Hellenic Foundation for Research and Innovation (HFRI) and the General Secretariat for Research and Technology (GSRT) under grant agreement no. [776] "PhotoDaLu" (KA97507). This research was co-financed by Greece and the European Union (European Social Fund – ESF) through the Operational Programme "Human Resources Development, Education and Lifelong Learning" in the context of the Act "Enhancing Human Resources Research Potential by undertaking a Doctoral Research" Sub-action 2: IKY Scholarship Programme for PhD candidates in the Greek Universities. The Chemistry Department of Aristotle University of Thessaloniki, Greece, is acknowledged for providing access to the Large Research Instrumentation single-crystal XRD Unit and NMR Unit. We thank Dr C. Gabriel of the HERACLES Research Center, KEDEK, Laboratory of Environmental Engineering (EnvE-Lab), Department of Chemical Engineering, Aristotle University of Thessaloniki, Greece, for using the LC-TOF mass spectrometer and performing the HRMS experiments.

References

1 S. A. Lawrence, *Amines: Synthesis, Properties and Applications*, Cambridge University Press, Cambridge, 2004.
2 D. Formenti, F. Ferretti, F. K. Scharnagl and M. Beller, *Chem. Rev.*, 2019, **119**, 2611–2680.
3 H. Göksu, H. Sert, B. Kilbas and F. Sen, *Curr. Org. Chem.*, 2017, **21**, 794–820.
4 M. Boronat, P. Concepción, A. Corma, S. González, F. Illas and P. Serna, *J. Am. Chem. Soc.*, 2007, **129**, 16230–16237.
5 S. Fountoulaki, V. Daikopoulou, P. L. Gkizis, I. Tamiolakis, G. S. Armatas and L. N. Lykakis, *ACS Catal.*, 2014, **4**, 3504–3511.
6 G. Zhang, F. Tang, X. Wang, L. Wang and Y.-N. Liu, *ACS Catal.*, 2022, **12**, 5786–5794.
7 G. Wu, M. Huang, M. Richards, M. Poirier, X. Wen and R. W. Draper, *Synthesis*, 2003, 1657–1660.
8 D.-Q. Xu, Z.-Y. Hu, W.-W. Li, S.-P. Luo and Z.-Y. Xu, *J. Mol. Catal. A: Chem.*, 2005, **235**, 137–142.
9 A. Corma and P. Serna, *Science*, 2006, **313**, 332–334.
10 J. Wu and C. Darcel, *Adv. Synth. Catal.*, 2023, **365**, 948–964.
11 S. Fu, N.-Y. Chen, X. Liu, Z. Shao, S.-P. Luo and Q. Liu, *J. Am. Chem. Soc.*, 2016, **138**, 8588–8594.
12 H.-U. Blaser, H. Steiner and M. Studer, *ChemCatChem*, 2009, **1**, 210–221.
13 J. Song, Z.-F. Huang, L. Pan, K. Li, X. Zhang, L. Wang and J.-J. Zou, *Appl. Catal., B*, 2018, **227**, 386–408.
14 J. F. Knifton, *J. Org. Chem.*, 1976, **41**, 1200–1206.
15 R. M. Deshpande, A. N. Mahajan, M. M. Diwakar, P. S. Ozarde and R. V. Chaudhari, *J. Org. Chem.*, 2004, **69**, 4835–4838.
16 G. Wienhöfer, M. Baseda-Krüger, C. Ziebart, F. A. Westerhaus, W. Baumann, R. Jackstell, K. Junge and M. Beller, *Chem. Commun.*, 2013, **49**, 9089–9091.
17 V. Zubar, A. Dewanji and M. Rueping, *Org. Lett.*, 2021, **23**, 2742–2747.
18 D. Timelthaler, W. Schöfberger and C. Topf, *Eur. J. Inorg. Chem.*, 2021, 2114–2120.
19 S. R. Boothroyd and M. A. Kerr, *Tetrahedron Lett.*, 1995, **36**, 2411–2414.
20 D. Wang and D. Astruc, *Chem. Rev.*, 2015, **115**, 6621–6686.
21 G. Wienhöfer, I. Sorribes, A. Boddien, F. Westerhaus, K. Junge, H. Junge, R. Llusar and M. Beller, *J. Am. Chem. Soc.*, 2011, **133**, 12875–12879.
22 U. Sharma, P. K. Verma, N. Kumar, V. Kumar, M. Bala and B. Singh, *Chem. – Eur. J.*, 2011, **17**, 5903–5907.
23 T.-Y. Hung, W.-S. Peng, J.-W. Tang and F.-Y. Tsai, *Catalysts*, 2022, **12**, 924–935.
24 B. G. Reed-Berendt, N. Mast and L. C. Morrill, *Eur. J. Org. Chem.*, 2020, 1136–1140.
25 Z. Shao, S. Fu, M. Wei, S. Zhou and Q. Liu, *Angew. Chem.*, 2016, **128**, 14873–14877.
26 H. S. Wilkinson, G. J. Tanoury, S. A. Wald and C. H. Senanayake, *Tetrahedron Lett.*, 2001, **42**, 167–170.
27 A. J. MacNair, M.-M. Tran, J. E. Nelson, G. U. Sloan, A. Ironmonger and S. P. Thomas, *Org. Biomol. Chem.*, 2014, **12**, 5082–5088.
28 K. Junge, B. Wendt, N. Shaikh and M. Beller, *Chem. Commun.*, 2010, **46**, 1769–1771.
29 L. Pehlivan, E. Métay, S. Laval, W. Dayoub, P. Demonchaux, G. Mignani and M. Lemaire, *Tetrahedron Lett.*, 2010, **51**, 1939–1941.
30 L. Pehlivan, E. Métay, S. Laval, W. Dayoub, P. Demonchaux, G. Mignani and M. Lemaire, *Tetrahedron*, 2011, **67**, 1971–1976.
31 P. K. Verma, M. Bala, K. Thakur, U. Sharma, N. Kumar and B. Singh, *Catal. Lett.*, 2014, **144**, 1258–1267.

This journal is © The Royal Society of Chemistry 2024

Open Access Article. Published on 21 2023. Downloaded on 2026/4/8 04:51:27.
This article is licensed under a Creative Commons Attribution-NonCommercial 3.0 Unported Licence.

32 J. Wu, S. Tongdee, Y. Ammaiyappan and C. Darcel, *Adv. Synth. Catal.*, 2021, **363**, 3859–3865.
33 S. Panda, A. Nanda, R. R. Behera, R. Ghosh and B. Bagh, *Chem. Commun.*, 2023, **59**, 4527–4530.
34 S. Sun, Z.-J. Quan and X.-C. Wang, *RSC Adv.*, 2015, **5**, 84574–84577.
35 R. Lopes, M. M. Pereira and B. Royo, *ChemCatChem*, 2017, **9**, 3073–3077.
36 R. R. Behera, S. Panda, R. Ghosh, A. A. Kumar and B. Bagh, *Org. Lett.*, 2022, **24**, 9179–9183.
37 U. Sharma, P. Kumar, N. Kumar, V. Kumar and B. Singh, *Adv. Synth. Catal.*, 2010, **352**, 1834–1840.
38 S. Yadav, S. Kumar and R. Gupta, *Inorg. Chem. Front.*, 2017, **4**, 324–335.
39 S. Kumar and R. Gupta, *ChemistrySelect*, 2017, **2**, 8197–8206.
40 D. I. Ioannou, D. K. Gioftsidou, V. E. Tsina, M. G. Kallitsakis, A. G. Hatzidimitriou, M. A. Terzidis, P. A. Angaridis and I. N. Lykakis, *J. Org. Chem.*, 2021, **86**, 2895–2906.
41 E. S. Raper, *Coord. Chem. Rev.*, 1996, **153**, 199–255.
42 E. S. Raper, *Coord. Chem. Rev.*, 1997, **165**, 475–567.
43 L. Gan, T. L. Groy, P. Tarakeshwar, S. K. S. Mazinani, J. Shearer, V. Mujica and A. K. Jones, *J. Am. Chem. Soc.*, 2015, **137**, 1109–1115.
44 Z. Han, L. Shen, W. W. Brennessel, P. L. Holland and R. Eisenberg, *J. Am. Chem. Soc.*, 2013, **135**, 14659–14669.
45 A. Das, Z. Han, W. W. Brennessel, P. L. Holland and R. Eisenberg, *ACS Catal.*, 2015, **5**, 1397–1406.
46 S. Seth, *Acta Crystallogr., Sect. C: Cryst. Struct. Commun.*, 1994, **50**, 1196–1199.
47 C. Fielding, S. Parsons and R. E. P. Winpenny, *Acta Crystallogr., Sect. C: Cryst. Struct. Commun.*, 1997, **53**, 174–176.
48 S. Dey, Md. E. Ahmed and A. Dey, *Inorg. Chem.*, 2018, **57**, 5939.
49 E. C. Constable, C. A. Palmer and D. A. Tocher, *Inorg. Chim. Acta*, 1990, **176**, 57–60.
50 O.-S. Jung, Y. T. Kim, Y.-A. Lee and H. K. Chae, *Bull. Korean Chem. Soc.*, 1998, **19**, 3.
51 S. Dey, T. K. Todorova, M. Fontecave and V. Mougel, *Angew. Chem., Int. Ed.*, 2020, **59**, 15726–15733.
52 A similar compound, containing the same cationic complex and Cl^- counter anion was recently reported by: M. E. Ahmed, A. Rana, R. Saha, S. Dey and A. Dey, *Inorg. Chem.*, 2020, **59**, 5292–5302.
53 M. G. Kallitsakis, D. I. Ioannou, M. A. Terzidis, G. E. Kostakis and I. N. Lykakis, *Org. Lett.*, 2020, **22**, 4339–4343.
54 A. Bhattacharjee, D. S. V. Brown, C. N. Virca, T. E. Ethridge, O. M. Galue, U. T. Pham and T. M. McCormick, *Dalton Trans.*, 2022, **51**, 3676–3685.
55 C. N. Virca and T. M. McCormick, *Dalton Trans.*, 2015, **44**, 14333–14340.
56 M. K. Awasthi, D. Tyagi, S. Patra, R. K. Rai, S. M. Mobin and S. K. Singh, *Chem. – Asian J.*, 2018, **13**, 1424–1431.
57 Z. Han, W. R. McNamara, M.-S. Eum, P. L. Holland and R. Eisenberg, *Angew. Chem., Int. Ed.*, 2012, **51**, 1667–1670.
58 S. Roy, B. Sharma, J. Pécaut, P. Simon, M. Fontecave, P. D. Tran, E. Derat and V. Artero, *J. Am. Chem. Soc.*, 2017, **139**, 3685–3696.
59 S. Kumar and R. Gupta, *Eur. J. Inorg. Chem.*, 2014, 5567–5576.
60 W. R. McNamara, Z. Han, C.-J. Yin, W. W. Brennessel, P. L. Holland and R. Eisenberg, *Proc. Natl. Acad. Sci. U. S. A.*, 2012, **109**, 15594–15599.
61 B. H. Solis and S. Hammes-Schiffer, *J. Am. Chem. Soc.*, 2012, **134**, 15253–15256.
62 W. Ai, R. Zhong, X. Liu and Q. Liu, *Chem. Rev.*, 2019, **119**, 2876–2953.
63 J. O. Bauer, G. Leitus, Y. Ben-David and D. Milstein, *ACS Catal.*, 2016, **6**, 8415–8419.
64 G. Albertin, S. Antoniutti, M. Bortoluzzi, A. Botter and J. Castro, *Inorg. Chem.*, 2016, **55**, 5592–5602.
65 M. J. Bezdek, S. Guo and P. J. Chirik, *Science*, 2016, **354**, 730–733.
66 L. D. Field, H. L. Li, S. J. Dalgarno and R. D. McIntosh, *Inorg. Chem.*, 2013, **52**, 1570–1583.
67 M. O. Konev, L. Cardinale and A. Jacobi von Wangelin, *Org. Lett.*, 2020, **22**, 1316–1320.